**Article ID:** 1000-324X(2013)10-1153-05 **DOI:** 10.3724/SP.J.1077.2013.13123

# Crystal Structure, Phase Transition and Optical Properties of ν-$PrBO_3$

JIN Teng-Teng[1,2], ZHANG Zhi-Jun[1], ZHANG Hui[1], ZHAO Jing-Tai[1]

(1. Key Laboratory of Transparent Opto-Functional Inorganic Materials of Chinese Academy of Sciences, Shanghai Institute of Ceramics, Chinese Academy of Sciences, Shanghai 200050, China; 2. University of Chinese Academy of Sciences, Beijing 100039, China)

**Abstract:** The praseodymium orthoborates λ-$PrBO_3$ and ν-$PrBO_3$ were synthesized from $Pr_6O_{11}$ and $H_3BO_3$ by solid state reaction method at 1200 and 1500℃, respectively. The crystal structure of ν-$PrBO_3$ was refined on the basis of single-crystal X-ray diffraction data. It crystallizes in the triclinic system belonging to space group $P\bar{1}$ with lattice parameters: $a$ = 0.6302 (4) nm, $b$ = 0.6521 (4) nm and $c$ = 0.6525 (4) nm, and $\alpha$ = 94.312(7)º, $\beta$ = 107.335(7)º, $\gamma$ = 106.455(7)º, $V$ = 0.2417(2) $nm^3$, $Z$ = 4. The phase transition process from λ-$PrBO_3$ to ν-$PrBO_3$ was also investigated. The optical band gaps of λ-$PrBO_3$ and ν-$PrBO_3$ are both determined to be about 4.96 eV according to the diffuse reflection spectra. There is no emission of $Pr^{3+}$ in the visible range for both of λ-$PrBO_3$ and ν-$PrBO_3$ under X-ray and UV excitation.

**Key words:** ν-$PrBO_3$ crystal structure; phase transition; optical properties

Over the last several decades, the rare-earth orthoborates $REBO_3$ have attracted a lot of attention owing to their extraordinary optical properties such as vacuum ultraviolet transparency and exceptional optical damage threshold[1-2]. It is well known that $REBO_3$ exhibits the related structure types as the three forms of $CaCO_3$, *i.e.*, aragonite, vaterite, and calcite[3]. $RE^{3+}$ adopt different coordination features depending on the size of the rare earth cations[4], but not with the above three forms at the same time. Most types of $REBO_3$ are designated with Greek letters in accordance with the nomenclature of Meyer[5-6]. In general, compounds containing larger ions (La-Nd, Sm, Eu), exhibit the aragonite-type structure (λ-$REBO_3$) at low temperature[3, 5], then transform to H-$REBO_3$ (RE=La, Ce, Nd)[7] and ν-$REBO_3$ (RE=Ce-Nd, Sm-Dy)[4-5, 8] at high temperature. However, compounds containing smaller ions exist as a low-temperature modification π-$REBO_3$ (RE =Y, Nd, Sm-Lu)[1, 3, 9-10] and a high-temperature modification μ-$REBO_3$ (RE =Y, Sm-Gd, Dy-Lu)[1, 10]. Although the high-temperature phases are different, they all exhibit low symmetry. For the smallest ion, $ScBO_3$ forms the calcite-type structure (β-$REBO_3$)[3, 11]. There are some other types of $REBO_3$ (RE =Er-Lu) which also adopt the same structure at low temperature. Additionally, the orthoborate phases χ-$REBO_3$ (RE = Dy and Er), which contain the new non-cyclic $[B_3O_9]^{9-}$ anion, were synthesized under high- pressure condition by Huppertz, *et al*[12], considered to be intermediates between the low-temperature ($\pi$) and high-temperature ($\mu$) polymorphs.

Due to the possible usage for fast scintillators, the $Pr^{3+}$-doped scintillators have attracted the attention of researchers recently, such as $Pr^{3+}$-doped single crystal hosts ($Y_3Al_5O_{12}$, $YAlO_3$ and $Y_2SiO_5$)[13-14]. This is because that the $Pr^{3+}$ ion can show even faster 5d-4f luminescence shifted by about 1.5 eV towards higher energies with respect to 5d-4f emission of $Ce^{3+}$[15].

In 1961, Levin, *et al*[3] reported the phase transitions of $REBO_3$ (RE=La, Sm, Nd), which occured at 1488, 1090 and 1285℃, respectively. The high temperature forms $NdBO_3$ and $SmBO_3$ are similar but different from $LaBO_3$. For the case of $PrBO_3$, there are few reports on phase transition process. According to previous studies[2, 6, 16-17], $PrBO_3$ mainly has two phases: the aragonite phase λ-$PrBO_3$ (low temperature, LT) and the triclinic phase ν-$PrBO_3$ (high temperature, HT). The two phases exhibit different structures and densities, and the crystal structure determination of λ-$PrBO_3$ from single crystals obtained through high-pressure and high-temperature synthesis method was reported in 2010[16]. However, the detailed crystal structure of ν-$PrBO_3$ is still unknown besides the cell parameters of ν-$PrBO_3$ reported by Meyer[6]. What's more, there is no report about the phase transition and optical properties of $PrBO_3$. In the present work, we focus on the investigation of the crystal structure of ν-$PrBO_3$, phase

**Received date:** 2013-03-06; **Modified date:** 2013-05-16; **Published online:** 2013-07-04
**Foundation item:** National Natural Science Foundation of China(11104298)
**Biography:** JIN Teng-Teng(1986–), female, PhD candidate. E-mail: ttjin2008@126.com
**Corresponding author:** ZHAO Jing-Tai, professor. E-mail: jtzhao@mail.sic.ac.cn

transformation from λ-$PrBO_3$ (LT) to ν-$PrBO_3$ (HT), as well as its optical properties.

# 1 Experiment

The λ-$PrBO_3$ (LT) and ν-$PrBO_3$ (HT) samples were both prepared by solid-state reaction in the muffle furnace. The starting materials were $Pr_6O_{11}$ (99.99%) and $H_3BO_3$ (99.99%). A stoichiometric mixture of the starting materials (with 10mol% excess of boric acid to compensate for its evaporation loss during heating) was ground in agate mortar. Then the mixed powders were loaded into platinum crucibles, and calcined in the furnace within air atmosphere at different temperatures. The λ-$PrBO_3$ (LT) sample was obtained at 1200℃ for 12 h, and the ν-$PrBO_3$ (HT) sample was obtained at 1500℃ for 5 h. Both powder samples were green. But there are some single crystals in powder ν-$PrBO_3$ (HT) sample.

The powder X-ray diffraction data for λ-$PrBO_3$ (LT) were collected at ambient temperature in air with a HUBER Imaging Plate Guinier camera G670 [S] (CuKα1 radiation, $\lambda$ = 0.154056 nm, Ge monochromator). The $2\theta$ range of all the data sets is from 5° to 100° with a step of 0.005°.

Single crystal X-ray diffraction data for ν-$PrBO_3$ (HT) were collected with CCD area detector (Mo Kα radiation, $\lambda$ = 0.071073 nm) at 293(2) K in the range of $3.31° < \theta < 24.98°$ using $\omega$ scan. Absorption correction was performed with a multi-scan procedure. The crystal structure refinement was performed by a full-matrix least-squares procedure within the SHELXS97 (Sheldrick, 1990)[18]. For crystal structure presentation the program Diamond 3.0 was used[19].

The Fourier transform infrared (FT-IR) spectra of ν-$PrBO_3$ were recorded at room temperature in the range of 400−1600 $cm^{-1}$ with a Spectrum 100 Optical (Perkin-Elmer).

The diffuse reflectance spectra of the samples were measured at room temperature by a Perkin Elmer LS 50B spectrophotometer equipped with a Xe flash lamp. The reflection spectra were calibrated with the reflection of black felt (reflection 3%) and white barium sulfate ($BaSO_4$, reflection~100%) in the wavelength region of 200−900 nm.

# 2 Results and Discussion

## 2.1 Phase transformation and the structure of the ν-$PrBO_3$

Crystal data for ν-$PrBO_3$: Triclinic, space group $P\bar{1}$ (no. 2), $a$ = 0.6302 (4) nm, $b$ = 0.6521 (4) nm and $c$ = 0.6525 (4) nm, and $\alpha$ = 94.312(7)º, $\beta$ = 107.335(7)º, $\gamma$ = 106.455(7)º, $V$ = 0.2417(2) $nm^3$, Z = 4, $M_r$ = 199.72, $D_{calcd}$ = 5.489 $g/cm^3$. A total of 1137 data were collected and merged to give 783 unique reflections ($R_{int}$ = 0.041) of which 624 were considered to be observed [$F^2 > 2\sigma(F^2)$]. Final $R_1$ = 0.046, $wR_2$ = 0.121, $S$ (goodness of fit) = 0.98 were obtained for all the data. It confirms that the lattice parameters decrease regularly from Pr, Sm to Dy, along with the size of the cations[4, 6]. Fractional atomic coordinates and isotropic or equivalent isotropic displacement parameters ($\times 10^{-2}$ $nm^2$) of ν-$PrBO_3$ are shown in Table 1. For the light atoms of O and B isotropic displacement parameters are used. Important distances (nm) and angles (°) of ν-$PrBO_3$ are given in Table S1. In the structure of ν-$PrBO_3$, the Pr atoms are coordinated by eight O atoms, and the B atoms are in a threefold planar coordination by three O atoms. Figure 1 is the perspective view of the structure of ν-$PrBO_3$ with distorted $PrO_8$ dodecahedron with Pr–O distances in the range of 0.2297 (11) to 0.2654 (12) nm. Each $PrO_8$ shares edges with four neighbors to build infinite double chains along the [110] direction. The $BO_3$ groups are regular, with average B–O distances in the range of 0.135(2) to 0.139(2) nm and O–B–O angles in the range of 116.3 (15) –126.0 (16)°.

The powder X-ray diffraction pattern of λ-$PrBO_3$ (Fig. S1) confirms the previous study since all diffractions peaks can be readily indexed to the pure orthorhombic-aragonite phase of $PrBO_3$ (ICSD# 421745) with the cell parameters $a$ = 0.81419 nm, $b$ = 0.57776 nm, $c$ = 0.50692 nm, $V$ = 0.2385 $nm^3$. As described by Haberer, *et al*[16], the aragonite $PrBO_3$ crystallizes in the orthorhombic Pnma space group with the structure composing of $PrO_9$ polyhedra and trigonal $BO_3$ groups. Each $PrO_9$ polyhedron shares edges with six other $PrO_9$ polyhedra and three $BO_3$ triangles. In addition, each $BO_3$ triangle shares edges with three $PrO_9$ polyhedra at the same time. By comparison of

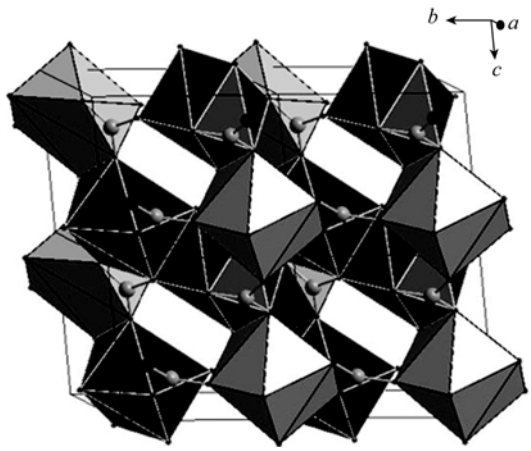


Fig. 1 Crystal structure of ν-$PrBO_3$
Grey and black polyhedra contain atoms Pr1 and Pr2, respectively

**Table 1 Fractional atomic coordinates and isotropic or equivalent isotropic displacement parameters ($\times10^{-2}$, $nm^2$) of single crystal ν-$PrBO_3$**

| Atom | *x* | *y* | *z* | $U_{iso}$*/$U_{eq}$ |
|---|---|---|---|---|
| Pr1 | 0.05468 (16) | 0.83915 (14) | 0.26610 (14) | 0.0070 (3) |
| Pr2 | 0.44039 (16) | 0.71637 (13) | −0.19427 (14) | 0.0061 (3) |
| O1 | 0.088 (2) | 0.8619 (18) | −0.3573 (19) | 0.008 (3)* |
| O2 | 0.376 (2) | 0.8827 (17) | 0.1295 (17) | 0.004 (2)* |
| O3 | 0.035 (2) | 0.5314 (18) | −0.2317 (18) | 0.008 (3)* |
| O4 | −0.147 (2) | 0.787 (2) | −0.134 (2) | 0.014 (3)* |
| O5 | 0.452 (2) | 0.7627 (19) | 0.4623 (19) | 0.011 (3)* |
| O6 | 0.625 (2) | 0.6681 (18) | 0.1987 (18) | 0.008 (2)* |
| B1 | 0.495 (3) | 0.774 (3) | 0.273 (3) | 0.007 (4)* |
| B2 | −0.018 (3) | 0.716 (3) | −0.244 (3) | 0.004 (4)* |

**Anisotropic atomic displacement parameters ($\times10^{-4}$, $nm^2$)**

| Atom | $U^{11}$ | $U^{22}$ | $U^{33}$ | $U^{12}$ | $U^{13}$ | $U^{23}$ |
|---|---|---|---|---|---|---|
| Pr1 | 0.80 (6) | 0.49 (5) | 1.03 (6) | 0.30 (4) | 0.50 (4) | 0.32 (4) |
| Pr2 | 0.65 (6) | 0.35 (5) | 0.98 (6) | 0.18 (4) | 0.42 (4) | 0.24 (4) |

* isotropic refined atoms

the two modifications, it is obvious that the Pr atoms in the high temperature phase has less coordination number of O than the low temperature phase, and each polyhedron share only 4 edges while 6 edges shared in the low temperature modification. This leads to the obvious changes of the lattice parameters.

According to the discussion above, it is possible that $PrBO_3$ compound exists in two different phases, *i.e.*, aragonite and triclinic phases. Since there are few reports on the structure phase transition process, it is more worth of notice. In order to study the relationship between the two phases, the sample λ-$PrBO_3$ synthesized at 1200℃ were annealed at 1200℃, 1300℃, 1400℃ and 1450℃ in air for 5 h, respectively. The results (Fig. 2) turn out that the phase transition point occurs around 1450℃. Since the transition between the two structure modifications did not follow group-subgroup relationship, it may be concluded that the phase transition is first order with reconstructive manner. The detailed mechanism of phase transition of $PrBO_3$ will be further investigated and published elsewhere.

## 2.2 FT-IR spectroscopy of ν-$PrBO_3$

To ascertain the structure of samples, corresponding FT-IR spectroscopy of samples were investigated. The FT-IR spectrum of ν-$PrBO_3$ in the range of 400–1600 $cm^{-1}$ is shown in Fig. 3.

According to the previous literatures, for an isolated planar trigonal $BO_3$ group, there are usually six fundamental modes of vibrations, which are symmetric stretch, $\nu_1$ (non degenerate, 950 $cm^{-1}$), out of plane bending, $\nu_2$ (non degenerate, 740 $cm^{-1}$), antisymmetric stretch, $\nu_3$ (doubly degenerate, 1250 $cm^{-1}$), plane bending, $\nu_4$ (doubly degenerate, 600 $cm^{-1}$)[20]. The observed vibration frequencies of ν-$PrBO_3$ are listed in Table S2 with their assignments. The modes of vibrations of ν-$PrBO_3$ are those typical for the isolated planar ion $BO_3$ as observed in $NdBO_3$ and $SmBO_3$[7]. Therefore, the result is consistent with its corresponding powder XRD data.

## 2.3 Diffuse reflection spectra of ν-$PrBO_3$ and λ-$PrBO_3$

The diffuse reflection spectrum of ν-$PrBO_3$ is recorded in the range of 230–700 nm (Fig. 4). The figure exhibits a

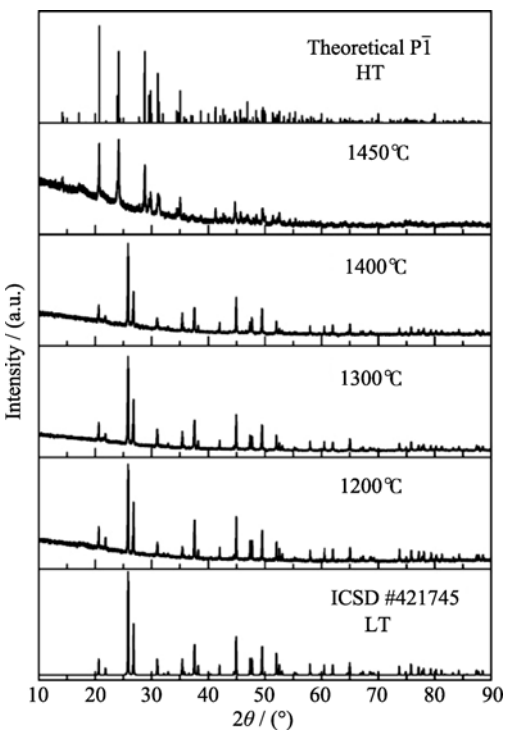


Fig. 2 XRD patterns of λ-$PrBO_3$ annealed in air at different temperatures

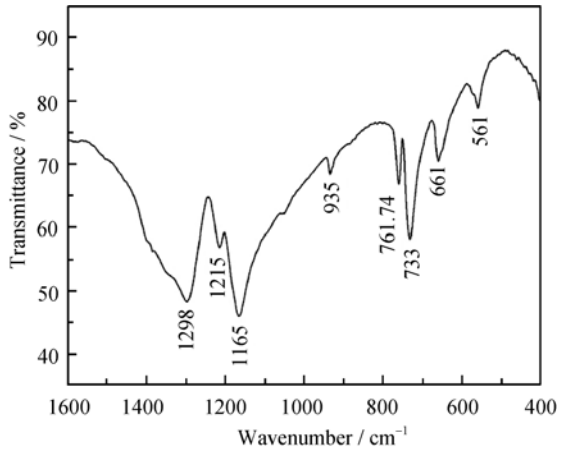


Fig. 3 FT-IR spectrum of ν-$PrBO_3$ in the range of 400–1600 $cm^{-1}$

drastic drop in the reflection in the UV range around 250 nm (4.96 eV), which defines the optical band gap of ν-$PrBO_3$ host lattice. It shows several absorption lines at long wavelength (*i.e.* low energy) in the range of 448–484 nm as well as 586–598 nm, which are ascribed to the typical f-f transitions from $^3H_4 \rightarrow {}^3P_2$ (~448 nm), $^3H_4 \rightarrow {}^3P_1$ (~474 nm), $^3H_4 \rightarrow {}^3P_0$ (~485 nm) and $^3H_4 \rightarrow {}^1D_2$ (~598 nm) of $Pr^{3+}$ ions, respectively. The absence of charge transfer band of $O^{2-}$-$Pr^{4+}$ rules out the possibility of $Pr^{4+}$ in ν-$PrBO_3$, indicating that all the Pr ions in ν-$PrBO_3$ exist in the trivalent state. The daylight color of ν-$PrBO_3$ shows light green as a result of the strong absorption by $Pr^{3+}$ in the visible range of 420–650 nm.

In order to better localize the thresholds for host lattice absorption and the absorption by $Pr^{3+}$, the absorption spectrum of ν-$PrBO_3$ was obtained from the reflection spectrum by using the Kubelka-Munk function[21]:

$$F(R) = (1-R)^2 / 2R = K / S$$

Where $R$, $K$, $S$ are the reflection, absorption coefficient, and scattering coefficients, respectively. The absorption ($K$/$S$) spectrum of ν-$PrBO_3$ derived with the Kubelka-Munk function is shown in the inset of Fig. 4. The value of the optical band gap of ν-$PrBO_3$ is calculated to be about 4.96 eV (*i.e.* 250 nm) by extrapolating the Kubelka-Munk function to $K/S = 0$.

Figure 5 shows diffuse reflection spectrum of λ-$PrBO_3$ under the same conditions as ν-$PrBO_3$. It shows no obvious change compared to ν-$PrBO_3$. The value of optical band gap of λ-$PrBO_3$ is also around 250 nm (4.96 eV), which is calculated from the absorption spectrum (the inset of Fig. 5).

The X-ray excited luminescence spectrum and photoluminescence spectra of λ-$PrBO_3$ and ν-$PrBO_3$ were measured. However, no emission of $Pr^{3+}$ in the UV-Vis range were observed in both of the two host lattices, probably due to the compositional quenching caused by high Pr content.

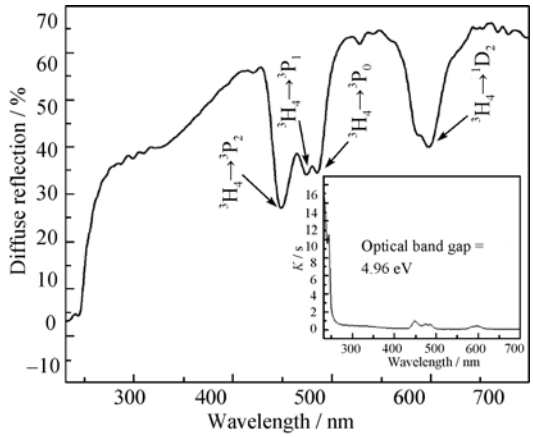


Fig. 4 Diffuse reflection spectrum of ν-$PrBO_3$
Inset shows the absorption spectrum of ν-$PrBO_3$ obtained from the reflection spectrum by using the Kubelka-Munk function

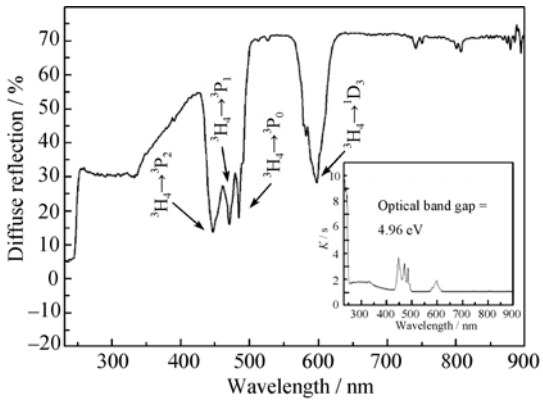


Fig. 5 Diffuse reflection spectrum of λ-$PrBO_3$
Inset shows the absorption spectrum of λ-$PrBO_3$ obtained from the reflection spectrum by using the Kubelka-Munk function

## 3 Conclusions

λ-$PrBO_3$ and ν-$PrBO_3$ were successfully synthesized by solid state method. The XRD results confirm that the high-temperature phase ν-$PrBO_3$ is isostructural with ν-$SmBO_3$, crystallizes in the triclinic system belonging to space group $P\bar{1}$. According to the XRD results, the phase transition temperature from λ-$PrBO_3$ to ν-$PrBO_3$ occurs at about 1450℃. The diffuse reflection spectrum of ν-$PrBO_3$ is also studied and its optical band gap is determined to be about 4.96 eV, which has no obvious change compared to λ-$PrBO_3$. PL and XEL studies of both phases show no emission at visible region.

## References:

[1] Lin J H, Sheptyakov D, Wang Y X, *et al.* Structures and phase transition of vaterite-type rare earth orthoborates: a neutron diffraction study. *Chem. Mater.*, 2004, **16(12):** 2418−2424.

[2] Pitscheider A, Kaindl R, Oeckler O, *et al*. The crystal structure of π-$ErBO_3$: new single-crystal data for an old problem. *J. Solid State Chem.*, 2011, **184(1):** 149−153.

[3] Levin E M, Roth R S, Martin J B. Polymorphism of $ABO_3$ type rare earth borates. *Am. Mineral.*, 1961, **46:** 1030−1055.

[4] Emme H, Huppertz H. High-pressure synthesis of ν-$DyBO_3$. *Acta Crystallogr., Sect. C: Cryst. Struct. Commun.*, 2004, **60:** I117−I119.

[5] Meyer H J. Rare earth orthoborates of aragonite structure. *Naturwissenschaften,* 1969, **56:** 458−459.

[6] Meyer H J. Triclinic orthoborates of rare-earths. *Naturwissenschaften,* 1972, **59:** 215.

[7] Lemanceau S, Bertrand-Chadeyron G, Mahiou R, *et al*. Synthesis and characterization of H-$LnBO_3$ orthoborates (Ln = La, Nd, Sm, and Eu). *J. Solid State Chem.*, 1999, **148(2):** 229−235.

[8] Noirault S, Joubert O, Caldes M T, *et al*. High-temperature form of neodymium orthoborate, $NdBO_3$. *Acta Crystallogr.*, *Sect. E: Struct. Rep. Online*, 2006, **62:** I228−I230.

[9] Newnham R E, Redman M J, Santoro R P. Crystal structure of yttrium and other rare-earth borates. *J. Am. Ceram. Soc.*, 1963, **46:** 253−256.

[10] Ren M, Lin J H, Dong Y, *et al*. Structure and phase transition of $GdBO_3$. *Chem. Mater.*, 1999, **11(6):** 1576−1580.

[11] Keszler D A, Sun H X. Structure of $ScBO_3$. *Acta Crystallogr., Sect. C: Cryst. Struct. Commun.*, 1988, **44:** 1505−1507.

[12] Huppertz H, Eltz B, Hoffmann R D, *et al*. Multianvil high-pressure syntheses and crystal structures of the new rare-earth oxoborates χ-$DyBO_3$ and χ-$ErBO_3$. *J. Solid State Chem.*, 2002, **166(1):** 203−212.

[13] van Eijk C W E, Dorenbos P, Visser R. $Nd^{3+}$ and $Pr^{3+}$ doped inorganic scintillators. *Nucl. Sci.*, 1994, **41(4):** 738−741.

[14] Gumanskaya E G, Egorycheva O A, Korzhik M V, *et al*. Spectroscopic properties and scintillation efficiency of cerium-doped $YAlO_3$ single crystals. *Opt. Spectrosk.*, 1992, **72(2):** 395−399.

[15] Dorenbos P. Systematic behaviour in trivalent lanthanide charge transfer energies. *J. Phys. Condens. Matter.*, 2003, **15:** 8417−8434.

[16] Haberer A, Kaindl R, Huppertz H. Synthesis and crystal structure of the praseodymium orthoborate λ-$PrBO_3$. *Z. Naturforsch., B: Chem. Sci.*, 2010, **65:** 1206−1212.

[17] Laperches J P, Tarte P. Spectres dabsorption infrarouge deborates deterres rares. *Spectrochim Acta*, 1966, **22:** 1201−1210.

[18] Sheldrick G M. SHELXL97, Release 97−2, University of Göttingen, Germany.

[19] Klaus Brandenburg, Diamond 3.0, 1997-2004, Crystal Impact GbR, Bonn, Germany.

[20] Velchuri R, Kumar B V, Devi V R, *et al*. Preparation and characterization of rare earth orthoborates, $LnBO_3$ (Ln = Tb, La, Pr, Nd, Sm, Eu, Gd, Dy, Y) and $LaBO_3$:Gd, Tb, Eu by metathesis reaction: ESR of $LaBO_3$:Gd and luminescence of $LaBO_3$:Tb, Eu. *Mater. Res. Bull.*, 2011, **46(8):** 1219−1226.

[21] Yamashita N. Luminescence centers of Ca(S:Se) phosphors activated with impurity ions having $S^2$ configuration. 1. Ca(S:Se):$Sb^{3+}$ phosphors. *J. Phys. Soc. Jpn.*, 1973, **35:** 1089−1097.

# *v*-$PrBO_3$ 的晶体结构、相变和光学性质

金滕滕 [1,2], 张志军 [1], 张 辉 [1], 赵景泰 [1]

(1.中国科学院 上海硅酸盐研究所, 中国科学院透明光功能无机材料重点实验室, 上海 200050; 2.中国科学院大学, 北京 100039)

**摘 要:** 采用高温固相合成法分别在 1200 和 1500℃合成了 λ-$PrBO_3$ 和ν-$PrBO_3$ 样品, 并通过单晶 X 射线衍射确定了ν-$PrBO_3$ 的晶体结构。结果表明该结构为三斜晶系, 空间群为 $P\bar{1}$, 晶胞参数为 $a$ = 0.6302 (4) nm, $b$ = 0.6521 (4) nm, $c$ = 0.6525 (4) nm, $\alpha$ = 94.312(7) º, $\beta$ = 107.335(7) º, $\gamma$ = 106.455(7) º, $V$ = 0.2417(2) $nm^3$, $Z$ = 4。同时研究了从 λ-$PrBO_3$ 到ν-$PrBO_3$ 的相变过程, 并从漫反射光谱得出 λ-$PrBO_3$ 和ν-$PrBO_3$ 的光学带隙均为 4.96 eV。在 X 射线和紫外激发下,均未观测到 λ-$PrBO_3$ 和ν-$PrBO_3$ 样品在紫外可见波长范围内的 $Pr^{3+}$特征发光。

**关　键　词:** ν-$PrBO_3$ 晶体结构; 相变; 光学性质

**中图分类号:** O78　　**文献标识码:** A

# Supporting Information

# Crystal Structure, Phase Transition and Optical Properties of ν-$PrBO_3$

JIN Teng-Teng[1,2], ZHANG Zhi-Jun[1], ZHANG Hui[1], ZHAO Jing-Tai[1]

(1. Key Laboratory of Transparent Opto-Functional Inorganic Materials of Chinese Academy of Sciences, Shanghai Institute of Ceramics, Shanghai 200050, China; 2. University of Chinese Academy of Science, Beijing 100039, China)

**Table S1 Important distances ($\times 10^{-1}$, nm) and angles (°) of single crystal ν-$PrBO_3$**

| Atoms | Distance and angle | Atoms | Distance and angle |
|---|---|---|---|
| Pr1—O3i | 2.297 (11) | Pr2—O5v | 2.304 (11) |
| Pr1—O1ii | 2.392 (11) | Pr2—O4vi | 2.414 (13) |
| Pr1—O2 | 2.398 (11) | Pr2—O6vii | 2.419 (11) |
| Pr1—O1iii | 2.470 (12) | Pr2—O3 | 2.422 (11) |
| Pr1—O4 | 2.487 (12) | Pr2—O2viii | 2.486 (11) |
| Pr1—O6iv | 2.505 (12) | Pr2—O2 | 2.496 (11) |
| Pr1—O4iii | 2.615 (12) | Pr2—O6 | 2.565 (11) |
| Pr1—O5 | 2.654 (12) | Pr2—O1 | 2.627 (12) |
| B1—O5 | 1.35 (2) | B2—O1 | 1.39 (2) |
| B1—O2 | 1.39 (2) | B2—O3 | 1.34 (2) |
| B1—O6 | 1.37 (2) | B2—O4 | 1.38 (2) |
| O5—B1—O6 | 126.0 (16) | O3—B2—O4 | 125.9 (15) |
| O5—B1—O2 | 116.4 (16) | O3—B2—O1 | 117.3 (15) |
| O6—B1—O2 | 117.1 (15) | O4—B2—O1 | 116.3 (15) |

Symmetry codes: (i) −x, −y+1, −z; (ii) x, y, z+1; (iii) −x, −y+2, −z; (iv) x−1, y, z; (v) x, y, z−1; (vi) x+1, y, z; (vii) −x+1, −y+1, −z; (viii) −x+1, −y+2, −z; (ix) −x, −y+2, −z+1.

**Table S2 Observed frequencies of the different vibration modes in ν-$PrBO_3$**

| Band/$cm^{-1}$ | Assignment ν(B−O) in $BO_3$ |
|---|---|
| 1298 | $\nu_3$ |
| 1215 | $\nu_3$ |
| 1165 | $\nu_3$ |
| 935 | $\nu_1$ |
| 762 | $\nu_2$ |
| 733 | $\nu_2$ |
| 661 | $\nu_4$ |
| 561 | $\nu_4$ |

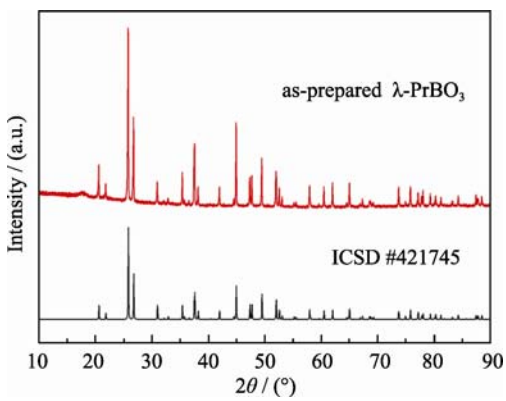


Fig. S1 The powder X-ray diffraction pattern of λ-$PrBO_3$